Overexpression of heme oxygenase-1 induced by constitutively activated NF-κB as a potential therapeutic target for activated B-cell-like diffuse large B-cell lymphoma

JUN HUANG[1-3], PENGXIANG GUO[5], DAN MA[1,4], XIAOJING LIN[1-3], QIN FANG[4] and JISHI WANG[1-3]

[1]Guizhou Medical University; [2]Department of Hematology, The Affiliated Hospital of Guizhou Medical University; [3]Guizhou Provincial Laboratory of Hematopoietic Stem Cell Transplantation Center; [4]Department of Pharmacy, The Affiliated Baiyun Hospital of Guizhou Medical University; [5]People's Hospital of Guizhou Province, Guiyang 550004, P.R. China

Received March 5, 2016; Accepted April 22, 2016

DOI: 10.3892/ijo.2016.3529

Abstract. There is an urgent requirement for a new therapeutic target for activated B-cell-like lymphoma (ABC-DLBCL), which is known to have dismal outcome and constitutive activation of NF-κB. Heme oxygenase-1 (HO-1) can inhibit apoptosis and promote proliferation in many cancers. To our knowledge, no studies have been performed on the correlation between HO-1 and DLBCL. In this study, immunohistochemical analysis of 31 tumor tissues from DLBCL patients [20 of ABC subtype and 11 of germinal center B-cell-like (GCB) subtype] and 11 normal lymph nodes revealed that HO-1 overexpression was characteristic of ABC-DLBCL. In addition, HO-1 mRNA expression levels were consistent with the immunohistochemistry results. High levels of HO-1 expression were significantly correlated with the involvement of more than 1 extranodal site (p=0.025), with a high positivity rate of Ki-67 (p<0.01). Similar to its anti-apoptotic role in other malignancies, HO-1 upregulation suppressed apoptosis of the ABC-DLBCL cell line OCI-ly10, whereas its downregulation sensitized the tumor cells to chemotherapeutic drugs. Further study demonstrated that the HO-1 overexpression was mediated by constitutively activated NF-κB which together played an anti-apoptotic role in ABC-DLBCL. Combination of the NF-κB inhibitor Bay11-7082 and the lentivirus vector Lenti-siHO-1 significantly decreased HO-1 protein expression and increased apoptosis in OCI-ly10 cells. However, in GCB-DLBCL cells with low levels of NF-κB expression, the TNF-α-mediated activation of NF-κB leading to HO-1 upregulation rescued the cells from apoptosis caused by HO-1 silencing. These results indicated that HO-1 can be a potential target for the treatment of ABC-DLBCL.

Correspondence to: Dr Jishi Wang, Guizhou Province Laboratory of Hematological Disease Diagnostic and Treat Centre, Department of Hematology, Affiliated Hospital of Guizhou Medical University, Guizhou Province Hematopoietic Stem Cell Transplantation Centre, Guiyang, Guizhou 550004, P.R. China
E-mail: wangjishi9646@163.com

Key words: heme oxygenase-1, nuclear factor-κB, activated B-cell-like lymphoma, therapeutic target, apoptosis

Introduction

Diffuse large B-cell lymphoma (DLBCL) is an aggressive and the most common subtype of non-Hodgkin lymphoma, accounting for 30-40% of all newly diagnosed cases (1). DLBCLs are highly heterogeneous at the molecular level (2); gene expression profiling studies have identified ≥2 major molecular subtypes of DLBCL, germinal center B-cell-like (GCB) and activated B-cell-like (ABC) DLBCL, which differ with respect to the expression of hundreds of genes and have distinct prognoses (3). The biggest difference between ABC-DLBCL and GCB-DLBCL is that the ABC subtype has a lower cure rate. Significantly, after R-CHOP treatment, the ABC subtype shows an inferior outcome compared with that of the GCB subtype (3-year progression-free survival, ~40% versus 75%; p<0.001) (4). Therefore, it is very important to find potential therapeutic targets for ABC-DLBCL.

Heme oxygenase-1 (HO-1), also known as heat shock protein 32, is a stress-related cytoprotective molecule that is expressed constitutively in various neoplastic cells (5). HO-1 can be strongly induced in response to cellular stress and oxidative stimuli, such as nitric oxide (6), heat shock (7), and inflammatory cytokines (8). Moreover, under pathological or stress conditions, increased HO-1 expression can lead to resistance to apoptosis, promotion of cell proliferation, and alleviation of inflammation (9).

Recently, the relationships between high HO-1 expression, drug resistance, and promotion of cell proliferation have been extensively studied (10-14). Our previous studies have shown that HO-1 is highly expressed in acute myelogenous leukemia (AML), myelodysplastic syndromes, and chronic myelogenous leukemia (CML) (15-19), confirming that HO-1 plays an important role as an anti-apoptotic molecule and could be a potential target for treatment. However, the role of HO-1 in DLBCL remains to be elucidated. In this study, based on analyses of its

protein and mRNA levels in 31 DLBCL patients, we found that HO-1 was characteristically overexpressed in ABC-DLBCLs.

ABC-DLBCL is characterized by constitutive activation of the nuclear factor-κB (NF-κB) pathway (20,21). NF-κB is a key transcription factor that promotes cell survival and proliferation, and inhibition of apoptosis (22,23). Targeting of NF-κB and its downstream genes can trigger apoptosis in ABC-DLBCL cells (20,24,25). However, NF-κB regulates hundreds of genes, not all of which have been thoroughly investigated.

Many studies have been performed to clarify the relationship between NF-κB and HO-1 in various diseases. Recently, several studies have indicated that NF-κB can induce the expression of HO-1 (26-28). Li *et al* demonstrated that NF-κB activation is important for the upregulation of HO-1 (29). Rushworth *et al* demonstrated that nuclear factor erythroid 2-related factor 2 (Nrf2) expression is regulated by high levels of nuclear NF-κB in AML cells (30) and that Nrf2 is found directly upstream of HO-1 (31,32). To the best of our knowledge, the relevance of NF-κB and HO-1 in DLBCLs has not yet been clarified. Considering the relationship between HO-1 and NF-κB, we hypothesized that the high level of HO-1 expression in ABC-DLBCL is due to the constitutive activation of NF-κB. Furthermore, the NF-κB-regulated HO-1 may play an anti-apoptotic role, which leads to the dismal therapeutic outcomes in ABC-DLBCL.

Therefore, we analyzed the influence of HO-1 on vincristine (VCR)- and/or dexamethasone (DXM)-induced proliferation inhibition and apoptosis in OCI-ly10 cells. An approach involving knockdown of HO-1 gene expression via lentivirus-mediated siRNA delivery and another involving HO-1 overexpression were used. Furthermore, we focused on whether HO-1 overexpression plays an anti-apoptotic role in ABC-DLBCL and explored the possible mechanism involved.

Materials and methods

Study cohort. From 2008 to 2013, 32 newly diagnosed patients with DLBCL who had not received therapy were included in the study. Their paraffin-embedded tissues and fresh-frozen tumor tissues were obtained from the files of the Affiliated Hospital of Guiyang Medical University after necessary informed consent and/or exemption had been acquired. All DLBCL diagnoses were made according to the World Health Organization classification system (33). After determining the cell-of-origin subtypes of DLBCL using formalin-fixed paraffin-embedded (FFPE) tissue as previously described (34), 20 patients were grouped into the ABC subtype and 11 patients into the GCB subtype; only 1 patient was considered to have an unclassified subtype and was excluded from the study. The 31 patients in the study included 19 males and 12 females, aged 20-90 years (median age, 58 years). All patients underwent surgical resection of tumor tissue. Eleven normal lymph nodes (confirmed as normal tissues by pathology) from non-tumor adjacent tissues of gastric cancer patients were also selected as negative controls and 5 spleen samples from healthy individuals were selected as the positive control. The study was approved by the institutional review board (Affiliated Hospital of Guiyang Medical University), and informed consent was obtained in accordance with the Declaration of Helsinki, prior to obtaining fresh tumor tissue in each case. Patient characteristics are summarized in Table I.

Cells. The human DLBCL cell lines OCI-ly10, OCI-ly19 were purchased from Deutsche Sammlung von Mikroorganismen und Zellkulturen. The cell lines were cultured at 37˚C in a 5% humidified atmosphere in RPMI-1640 medium supplemented with 20% fetal bovine serum (Gibco BRL; Life Technologies, Carlsbad, CA, USA), penicillin (100 U/ml), and streptomycin (100 μg/ml). Normal human B lymphocytes were purified from blood donor buffy coats using the human B-cell enrichment cocktail from StemCell Technologies.

Reagents. The following reagents were used: fetal bovine serum (Gibco BRL); RPMI-1640 medium (Gibco BRL); dimethyl sulfoxide (DMSO; Sigma-Aldrich, St. Louis, MO, USA); Annexin V-fluorescein isothiocyanate (FITC)/propidium iodide (PI) apoptosis detection kit (BD Biosciences, San Jose, CA, USA); primary antibodies such as p-p65^{S536} and p-IκB-α$^{S32/S36}$ for western blot analysis (Cell Signaling Technology, Beverly, MA, USA); secondary antibodies (Li-Cor Corp., Lincoln, NE, USA); TRIzol reagent (Life Technologies); and VCR and DXM (Sigma-Aldrich).

Immunohistochemistry. Immunohistochemistry was performed on the study cohort samples obtained from the archives of Affiliated Hospital of Guiyang Medical University, using 5-μm-thick FFPE tissue sections. Slides were deparaffinized and pretreated with 10 mM citrate (pH 6.0; Zymed, South San Francisco, CA, USA) in a steam pressure cooker (Decloaking Chamber; BioCare Medical, Walnut Creek, CA, USA) and subsequently washed in distilled water. All further steps were performed at room temperature in a hydrated chamber. Slides were pretreated with Peroxidase Block (Dako USA, Carpinteria, CA, USA) for 5 min to quench endogenous peroxidase activity. Primary mouse anti-HO-1 antibody (1:120 dilution; Beyotime, Shanghai, China) was incubated in the Dako diluent (Dako USA) for 1 h. The specificity of the HO-1 antibody was previously confirmed by immunoblotting an HO-1-positive control cell line, demonstrating reactivity with a single band of appropriate molecular weight. Slides were washed in 50 mM Tris (Tris(hydroxymethyl) aminomethane)-Cl (pH 7.4) and incubated with anti-mouse horseradish peroxidase (HRP)-conjugated antibody solution (Envision+ Detection kit; Dako USA) for 30 min. After further washing, immunoperoxidase staining was developed with the chromogen diaminobenzidine (Dako USA), and slides were counterstained with Harris hematoxylin (Polyscientific, Bay Shore, NY, USA).

Quantitative analysis and staining interpretation. In order to evaluate HO-1 expression, immunostained sections were scored semiquantitatively according to the proportion of tumor cells stained and the staining intensity, as previously described (35,36). Briefly, all specimens were assessed using the immunoreactive score (IRS), which was calculated by multiplying the staining intensity (grade 0, none; 1, weak; 2, moderate; 3, strong) by the percentage of positively stained cells (0, <5.0%; 1, 5-25%; 2, 26-50%; 3, >51%). For HO-1 staining, samples with staining intensity greater than or equal

Table I. Clinical characteristics of diffuse large B-cell lymphoma patients.

Characteristic	n (%)
Median age, years	58
Clinical stage III, IV	16 (51.6)
Entranodal sites >1	13 (41.9)
ECOG PS ≥2	12 (38.7)
Lactate dehydrogenase > 1N	17 (54.8)
B symptoms present	19 (61.3)
Ki-67 ≥50%	21 (67.7)
IPI score	
Low (0-1)	11 (35.4)
Low intermediate (2)	6 (19.4)
High intermediate (3)	8 (25.8)
High (4-5)	6 (19.4)
Subtype	
Activated B-cell-like	20 (64.5)
Germinal center B-cell-like	11 (35.5)

ECOG PS, performance status according to the Eastern Cooperative Oncology Group scale; IPI, International Prognostic Index.

to the median value were categorized as high, whereas those with staining intensity lesser than the median value were categorized as low. We defined IRS ≥4 as positive and IRS <4 as negative.

For each tumor section, 5 randomly chosen fields and ≥500 cancer cells were analyzed. Slides were examined using an E-400 microscope (Nikon, Tokyo, Japan) to produce digital images that were visualized using a computer-aided image analysis system (Win ROOF version 5.0; Mitani, Fukui, Japan). Slides were evaluated twice at different times by 2 investigators who were blinded to the clinicopathological features and survival data.

Viral transduction. Sequences containing human HO-1 (HO-1, 5'-GCGTTTACCCGCCATCCGCACCCTAGGAGATCTCAGCCACAG-3') and small interfering RNA targeting human HO-1 (siRNA-HO-1, 5'-TGGTAGGGCTTTATGCCATGTTTCAAGAGAACATGGCATAAAGCCCTACTTTTTTC-3') were selected with Invitrogen designer software. Retroviruses were generated by transfecting empty plasmid vectors containing enhanced green fluoresence protein (EGFP) or vectors containing human HO-1-EGFP/siRNA-HO-1-EGFP into 293FT packaging cells, using FuGENE HD6. Lentiviral stocks were concentrated using the Lenti-X concentrator, and titers were determined with the Lenti-X qRT-PCR Titration kit (Shanghai Innovation Biotechnology Co., Ltd., China). Finally, 4 recombinant lentiviral vectors were constructed: lentivirus-V5-D-TOPO-HO-1-EGFP (L-HO-1), lentivirus-V5-D-TOPO-EGFP (TOPO-EGFP), lentivirus-pRNAi-U6.2-EGFP-siHO-1 (siHO-1), and lentivirus-pRNAi-U6.2-EGFP (RNAi-EGFP). For transduction, cells were plated onto 12-well plates at $2.5x10^5$ cells/well and infected with the lentiviral stocks at a multiplicity of infection of 10 in the presence of polybrene (10 μg/ml) and then analyzed by fluorescence microscopy (Olympus, Tokyo, Japan) and western blotting at 48 h post-transduction. OCI-ly10 cells and OCI-ly19 cells were transduced with L-HO-1, siHO-1, RNAi-EGFP and TOPO-EGFP, respectively.

MTT assay. The effects of HO-1 on the proliferation of OCI-ly10 cells, as well as the responses to VCR and DXM, were determined by using the 3-(4,5-dimethylthiazol-2-yl)-2,5-diphenyltetrazolium bromide (MTT) assay. Cells were seeded in 96-well plates at a density of 5,000 cells/well. The cell line was exposed to different concentrations of DXM (0.5, 1, 2, 4, 6, 8, 10 and 12 mM) and VCR (0.025, 0.05, 0.1, 0.2, 0.4, 0.8, 1.6 and 3.2 μM) for 24 h. After the treatment, 20 μl of MTT dye (5 mg/ml; Sigma-Aldrich) was added to each well. After 4 h of incubation at 37˚C, the culture medium was removed. Subsequently, 150 μl of DMSO was added and thoroughly mixed for 10 min. Spectrometric absorbance at 570 nm was measured with a microplate reader. The experiments were performed 5 times for each group. The survival rate (SR) was measured using the following equation: SR (%) = ($A_{Treatment}$/$A_{Control}$) x 100%. The concentration that produced 50% cytotoxicity (IC_{50}) was determined using GraphPad Prism 5.0 software (GraphPad Software Inc., San Diego, CA, USA).

Flow cytometry. Cells were harvested, washed with phosphate-buffered saline (PBS), and stained with an Annexin V-FITC/PI apoptosis kit (BD Biosciences) according to the manufacturer's instructions. Apoptotic cells were detected using a FACScan flow cytometer (Becton-Dickinson, Franklin Lakes, NJ, USA), and the data were analyzed using CellFIT software.

RNA extraction and qPCR. Total RNA was extracted from FFPE tissue sections of samples obtained from DLBCL patients by using the RNAprep Pure FFPE kit (TianGen Biotech, Beijing, China) according to the manufacturer's instructions. Total RNA from OCI-ly10 cells was extracted using TRIzol reagent according to the manufacturer's instructions. qPCR was performed using the SYBR Green PCR Master Mix (TianGen Biotech) and PRISM 7500 Real-Time PCR detection system (ABI PRISM, USA). The HO-1 expression level was analyzed relative to that of the β-actin gene. Primers for qPCR were as follows: HO-1-F, 5'-ACCCATGACACCAAGGACCAGA-3'; HO-1-R, 5'-GTGTAAGGACCCATCGGAGAAGC-3'; β-actin-F, 5'-GAGACCTTCAACACCCCAGC-3'; and β-actin-R, 5'-ATGTCACGCACGATTTCCC-3'. The reaction mixture contained cDNA, primers, and SYBR Master Mix and had a total volume of 20 μl. The thermal cycling conditions used were 1 min at 94˚C, followed by 40 cycles at 94˚C for 10 sec and 60˚C for 15 sec.

Immunofluorescence staining. The correlationship of p65 and HO-1 was examined by immunofluorescence. OCI-ly10 cells were plated on 6-well culture plates, Bay11-7082 pretreated or left untreated for 1 h, and incubated with TNF-α (15 ng/ml). Then the cells were rinsed in PBS and fixed by incubation with 4% formaldehyde in PBS for 15 min at room temperature. After washing with PBS, cells were permeabilized with PBS containing 0.25% Triton X-100. The cells were blocked in PBS containing 5% BSA for 30 min. Next, with further washing,

cells were incubated with a rabbit anti-HO-1 monoclonal antibody and a mouse anti-p65 monoclonal antibody, diluted at 1:200 with confining liquid, for 2 h at room temperature. After washing with PBS, cells were incubated with CY3-conjugated goat anti-mouse antibody (1:200) and FITC-conjugated goat anti-rabbit antibody (1:200) for 30 min, respectively. Then, the nucleus was stained with DAPI (4,6-diamidino-2-phenylindole) and cells were photographed by fluorescent microscopy.

Western blot analysis. To analyze fresh tumor tissues, proteins were extracted from a total of $5x10^6$ cells. To analyze the suspended cells, proteins were extracted from a total of $2x10^7$ cells. Total proteins were extracted by lysing cells in RIPA buffer containing 1 mM phenylmethanesulfonyl fluoride (Solarbio Science & Technology, Beijing, China). Cytoplasmic and nuclear proteins were extracted using a nuclear and cytoplasmic protein extraction kit (Beyotime) according to the manufacturer's instructions. Equal amounts of protein from the lysates were resolved using 10% SDS-PAGE gels and transferred to polyvinylidene difluoride membranes (Millipore Corp., Milford, MA, USA) in order to analyze protein expression by western blot analysis. The membranes were blocked with 5% non-fat milk in Tris-buffer at room temperature for 2 h and then incubated overnight at 4˚C with primary antibody against the protein of interest. After the membrane was washed with PBS with 0.1% Tween-20, it was incubated with the appropriate HRP-conjugated secondary antibody, and protein levels were detected with enhanced chemiluminescence (7Sea Biotech). The optical densities were analyzed using Quantity One software.

Statistical analysis. Statistical analysis of the data was conducted using SPSS version 19 software package (SPSS, Chicago, IL, USA). All data are presented as the mean ± standard error of the mean (SEM). Statistical analyses were performed using analysis of variance (ANOVA) and Student's t-test. The Fisher's exact test was used to assess the relationship between HO-1 expression and clinicopathological features. The optical density for the western blot assay was quantified with Quantity One software. A p-value of <0.05 was considered statistically significant.

Results

HO-1 is characteristically overexpressed in ABC-DLBCL patients. Upon immunohistochemical analysis of surgical resections of DLBCL tissues and normal lymph nodes, HO-1 expression was mainly detected in the cytoplasm and membrane of tumor cells, whereas nuclear staining was almost undetectable (Fig. 1A). The mean IRS was 4, and samples were considered positive when IRS was ≥4. Finally, 18 of 31 (58.1%) patients were found to have tumors positive for HO-1 expression, whereas normal lymph nodes were negative for HO-1 expression. Among these positive samples, we found that there was a significantly higher percentage of HO-1 positivity in ABC-DLBCL (75%) than in GCB-DLBCL (27.3%) (p=0.021). We also detected HO-1 mRNA expression in FFPE tissue sections, and the data showed that the expression of HO-1 was significantly higher in ABC-DLBCL than in GCB-DLBCL (p<0.01) and the negative control group (p<0.01) (Fig. 1B).

Table II. Correlation between HO-1 expression and clinicopathological features of DLBCL patients.

Characteristics	No. n=31	HO-1 expression		p-value
		Negative n=13	Positive n=18	
Age, years; n (%)				0.717
≤60	17	8 (47.1%)	9 (52.9%)	
>60	14	5 (35.7%)	9 (64.3%)	
Gender				0.689
Female	8	4 (50.0%)	4 (50.0%)	
Male	23	9 (39.1%)	14 (60.9%)	
Performance status				0.262
<2	19	6 (31.6%)	13 (68.4%)	
≥2	12	7 (58.3%)	5 (41.7%)	
T stage				0.285
I or II	15	8 (53.3%)	7 (46.7%)	
III or IV	16	5 (31.3%)	11 (68.8%)	
Extranodal sites involved				0.025
1 site	18	11 (61.1%)	7 (38.9%)	
>1 site	13	2 (15.4%)	11 (84.6%)	
LDH level[a]				0.703
Normal	12	4 (33.3%)	8 (66.7%)	
High	17	8 (47.1%)	9 (52.9%)	
IPI				0.275
Low to low-intermediate	17	9 (52.9%)	8 (47.1%)	
High-intermediate to high	14	4 (28.6%)	10 (71.4%)	
B symptoms				0.710
Absent	12	6 (50.0%)	6 (50.0%)	
Present	19	7 (36.8%)	12 (63.2%)	
Ki-67 expression[b]				<0.01
Positive	21	4 (19.0%)	17 (81.0%)	
Negative	10	9 (90.0%)	1 (10.0%)	
Subtype				0.021
ABC	20	5 (25.0%)	15 (75.0%)	
GCB	11	8 (72.7%)	3 (27.3%)	

[a]LDH categorization is based on the range for normal values in the clinical laboratory at our institution. LDH levels were missing in 2 patients but both patients had a total IPI score of 4 and were categorized in the high-risk group. [b]Ki-67 was judged to be positive when Ki-67 ≥50%.

These results indicated that high HO-1 expression is characteristic of ABC-DLBCL.

HO-1 expression correlates strongly with Ki-67 expression in DLBCL patients. HO-1 protein expression in DLBCL patients was further evaluated according to the clinicopathological characteristics of DLBCL; the results are summarized in Table II. Age and gender were not determinant factors of

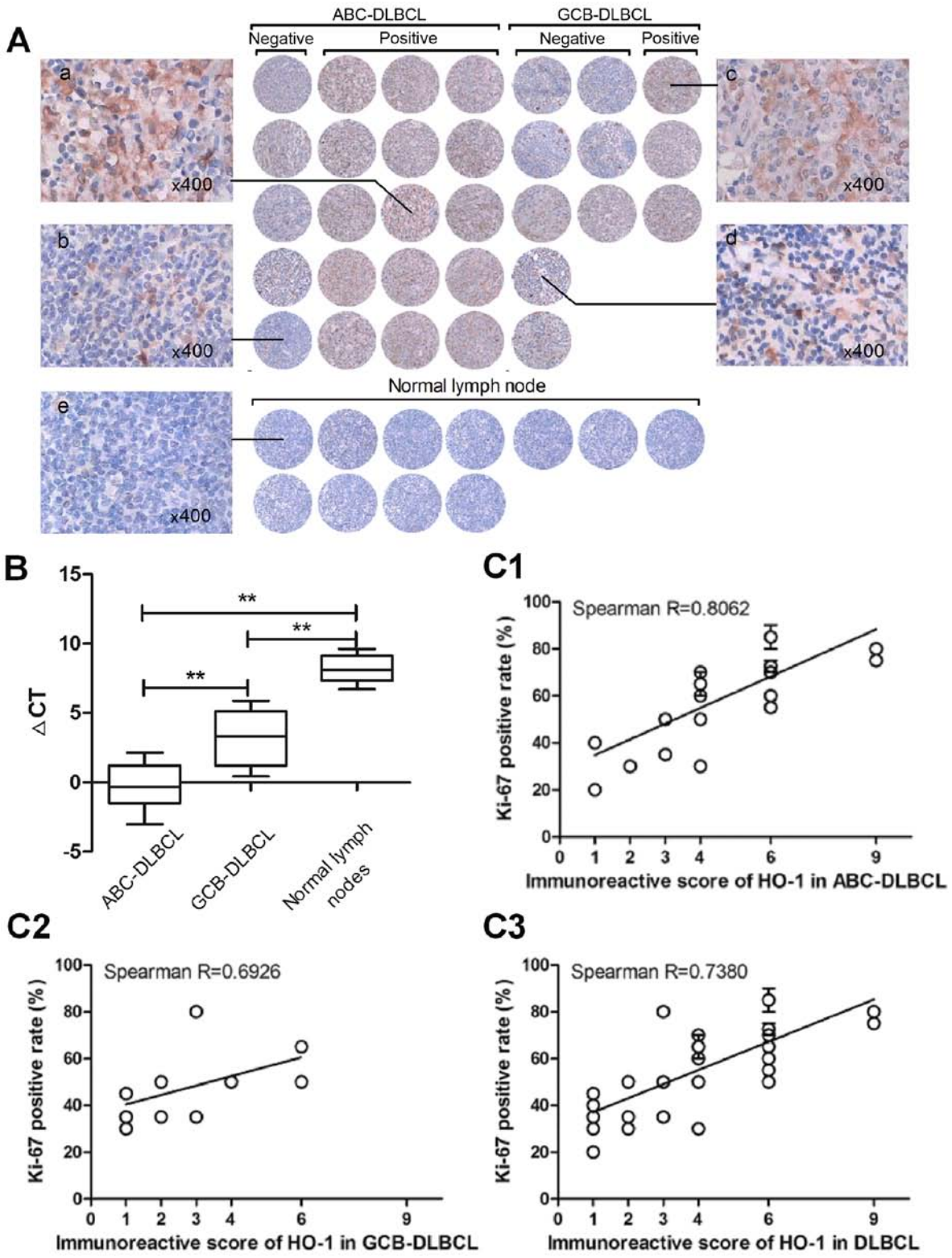

Figure 1. HO-1 is overexpressed in most ABC-DLBCL patients. (A) Overview of the immunohistochemical results for the 31 diffuse large B-cell lymphoma (DLBCL) tissue samples. Each field of view was ≥60% of the original image (x200). Labels a and c are representative cases of DLBCL-positive for HO-1 expression, b and d are representative cases of DLBCL-negative for HO-1 expression, and e is representative case of normal lymph nodes. (B) Differential expression of HO-1 mRNA in 31 DLBCL patients and 11 normal lymph nodes, as determined by qPCR. Data are presented as the ΔCT of HO-1 expression in the patient samples, with higher ΔCTs indicating lower expression. $^{**}p<0.01$. (C) Scatterplot representing the correlation of HO-1 expression with the Ki-67 positive rate in DLBCL, GCB-DLBCL and in ABC-DLBCL patient samples. Spearman correlation coefficient R for HO-1 positivity degree versus Ki-67 positive rate: in DLBCL, R=0.7380, p<0.01; in ABC-DLBCL, R=0.8062, p<0.01; in GCB-DLBCL, R=0.6926, p<0.01.

HO-1 expression. The rate of HO-1 positivity was significantly higher in patients with >1 site of extranodal involvement (11/13, 84.6%) than in patients with only 1 site of extranodal involvement (7/18, 38.9%) (p=0.025). However, no significant

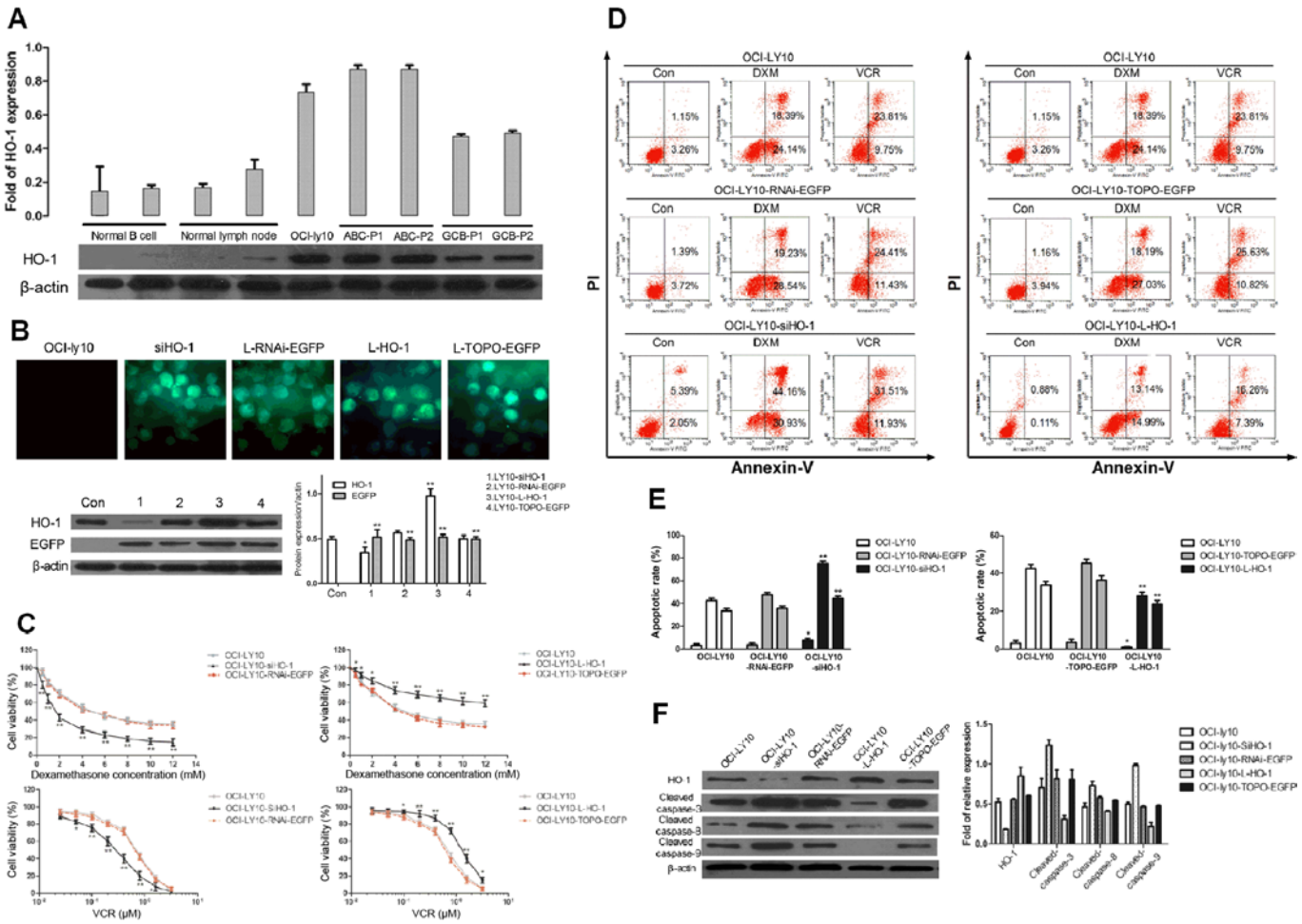

Figure 2. High expression of HO-1 can inhibit apoptosis of OCI-ly10 cells. (A) Western blot analysis of protein levels of HO-1 in OCI-ly10 cells and fresh frozen tissues from randomly selected diffuse large B-cell lymphoma patients. (B) Positivity of lentivirus-mediated HO-1 and siHO-1 transductions (>95%) observed by fluorescence microscopy. Expression of HO-1 after transduction was detected by western blotting. $^{**}p<0.01$ and $^{*}p<0.05$. (C) Transduced cells were treated with different doses of vincristine (VCR) or dexamethasone (DXM) for 24 h. Viability was evaluated by MTT assay. $^{**}p<0.01$ and $^{*}p<0.05$. (D) Apoptotic rates were detected by flow cytometry. (E) The data statistics of apoptosis in transduced cells. All experiments were repeated 3 times. $^{**}p<0.01$ and $^{*}p<0.05$. (F) Total protein was extracted from the different cell groups after treatment with 0.5 μM vincristine for 24 h, and the expression levels of HO-1, cleaved caspase-3, cleaved caspase-8, and cleaved caspase-9 were detected.

correlation was observed between the T stage and International Prognostic Index (IPI) score, performance status, lactate dehydrogenase levels, and B symptoms. The HO-1 positivity rate was strongly related with Ki-67 expression in DLBCL patients (R=0.7380; p<0.01). We then further analyzed the relationship between the expression of HO-1 and Ki-67 in ABC-DLBCLs and observed a more obvious correlation (R=0.8062; p<0.01) (Fig. 1C).

High expression of HO-1 can inhibit apoptosis in the ABC-DLBCL cell line OCI-ly10. Given a previous study showing that HO-1 expression and the Ki-67 positivity rate were closely related, and since Ki-67 is a proliferation-associated nuclear antigen (37), we concluded that HO-1 plays a role in promoting proliferation and preventing apoptosis, as previously described (5,9). HO-1 expression was compared among the ABC-derived cell line OCI-ly10, other different groups of cell lines, and cancer cells from randomly selected DLBCL patients. Western blot analysis showed that HO-1 was expressed at low levels in normal B cells, normal lymph nodes, and GCB-DLBCL cells, whereas ABC-DLBCL cells and OCI-ly10 cells had high levels of HO-1 expression (Fig. 2A).

In order to further investigate the effects of HO-1 on apoptosis, we used a lentiviral system to regulate HO-1 expression. Expression of HO-1 in OCI-ly10 cells was downregulated upon transduction with siHO-1 and upregulated upon transduction with L-HO-1. Western blotting results showed that HO-1 was highly expressed in OCI-ly10-Lentivirus-V5-D-TOPO-HO-1-EGFP (OCI-ly10-L-HO-1) cells but poorly expressed in OCI-ly10-lentivirus-pRNAi-U6.2-EGFP-siHO-1 (OCI-ly10-siHO-1) cells after 48 h of transduction, which indicates successful transductions of the vectors (Fig. 2B).

Subsequently, we examined the viability of OCI-ly10 cells in response to varying concentrations of DXM and VCR, which are commonly used chemotherapeutic drugs in DLBCLs. OCI-ly10, OCI-ly10-L-HO-1, OCI-ly10-TOPO-EGFP, OCI-ly10-siHO-1, and OCI-ly10-RNAi-EGFP cells were cultured with DXM and VCR at different concentrations. With increasing concentration of DXM or VCR, the viability of cells decreased gradually. At the same concentration of

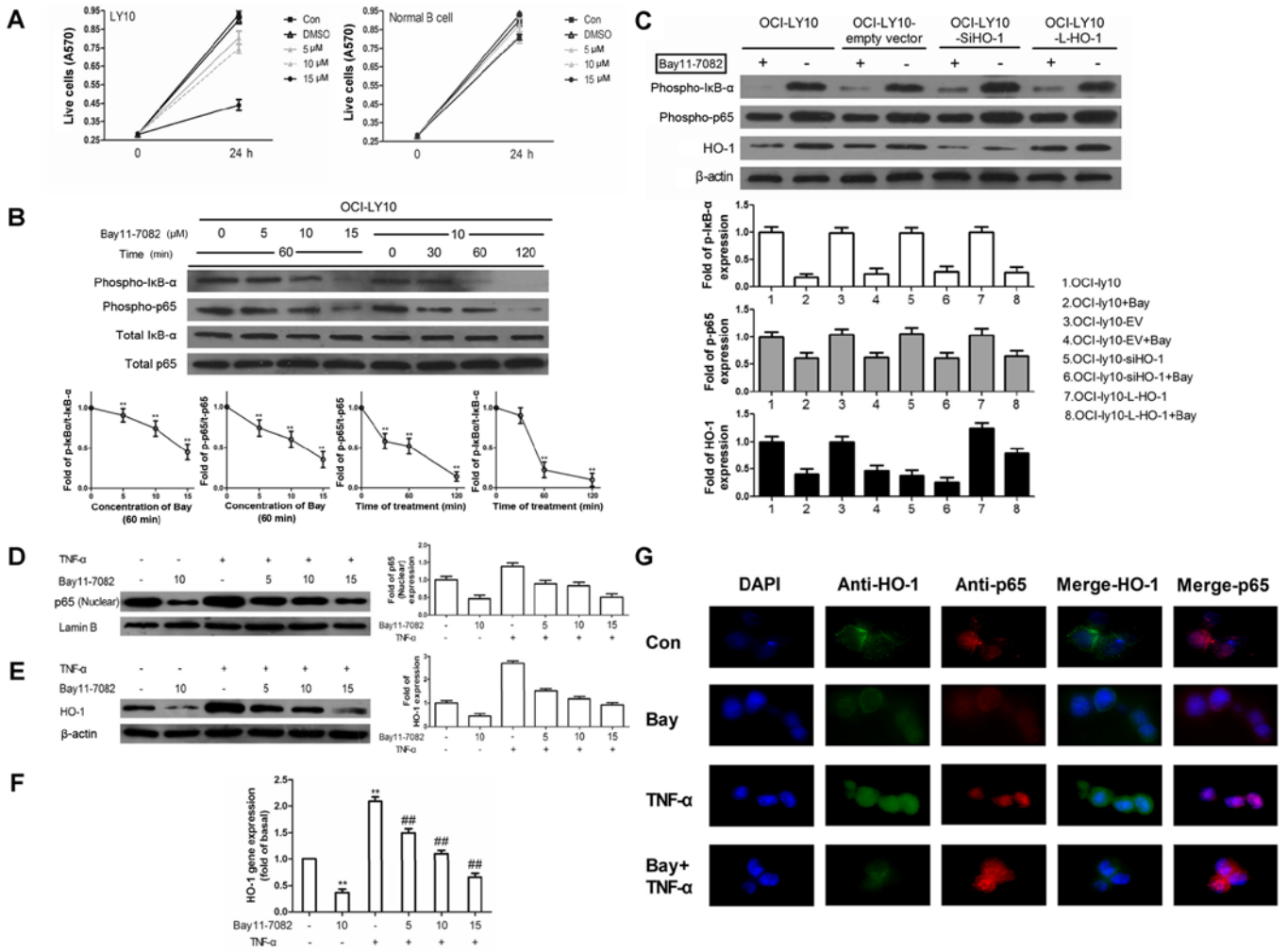

Figure 3. HO-1 overexpression is due to constitutively activated NF-κB in ABC-DLBCL. (A) MTT assays indicated that Bay11-7082 selectively reduced the growth of ABC-DLBCL cells (OCI-ly10) and did not affect human normal B cells. (B) Western blot analysis showed that Bay11-7082 treatment inhibited the phosphorylation of IκB-α and p65 (p-p65 and p-IκB-α) but not total-p65 or total-IκB-α (t-p65 and t-IκB-α) in OCI-ly10 cells. Cells were treated with the indicated drug concentrations and sampled at the indicated time-points. (C) Transduced OCI-ly10 cells were treated with or without Bay11-7082 at the indicated time-points and concentrations. Western blot assay for HO-1, p-p65, and p-IκB-α protein expression. (D-F) TNF-α induces NF-κB-dependent HO-1 increase in OCI-ly10 cells. (D) OCI-ly10 cells were pretreated with Bay11-7082 for 1 h and then incubated with TNF-α (15 ng/ml) for 15 min. The nuclear fractions were analyzed by western blotting using anti-p65 and anti-lamin B antibodies. (E) OCI-ly10 cells were pretreated with Bay11-7082 for 1 h and then incubated with TNF-α (15 ng/ml). Expression of HO-1 was detected by western blot analysis. (F) Quantitative PCR shows that the TNF-α-induced HO-1 mRNA increase was decreased by Bay11-7082. $^{**}p<0.01$ versus control; $^{\#\#}p<0.01$ versus TNF-α treatment. (G) To determine the effect of Bay11-7082 and TNF-α on p65 translocation and HO-1 expression, cells were pretreated with or without Bay11-7082 for 1 h and then treated with or without TNF-α (15 ng/ml). The translocation of p65 and the expression of HO-1 were determined by immunofluorescence staining (original magnification, x1,000). The merged images were obtained after superposition of the green (HO-1) and blue (DAPI) channels or the red (p65) and blue (DAPI) channels. The images are representative of 3 separate experiments.

DXM or VCR, cells with a high HO-1 expression level had significantly higher viability rates than their counterparts with low expression (Fig. 2C). The apoptosis rate of high HO-1-expressing groups was the lowest, whereas that of low HO-1-expressing groups was the highest. These results were validated by the Annexin V-FITC/PI assay after induction of cells with 1 mM DXM or 0.5 μM VCR for 24 h (Fig. 2D). Interestingly, HO-1 expression was negatively correlated with the expression of apoptotic proteins, including cleaved caspase-3, cleaved caspase-8, and cleaved caspase-9, when cells were treated with 0.5 μM VCR (Fig. 2F). Hence, these data demonstrate that upregulation of the HO-1 expression can lead to the inhibition of OCI-ly10 cell apoptosis, indicating that HO-1 has an anti-apoptotic effect.

Characteristic HO-1 overexpression in ABC-DLBCL is driven by constitutively activated NF-κB. Having confirmed that HO-1 is associated with apoptosis, the next step was to investigate the mechanism of the HO-1 expression increase in ABC-DLBCL. Previous studies indicated that HO-1 expression is regulated by NF-κB (26-29). Because NF-κB is known to be constitutively activated in ABC-DLBCL, we hypothesized that the characteristic HO-1 overexpression in ABC-DLBCL could be regulated by NF-κB.

To test this hypothesis, we treated OCI-ly10 cells with Bay11-7082, an inhibitor of IκB-α phosphorylation. Bay11-7082 inhibited the phosphorylation of IκB-α and p65 in a time- and dose-dependent manner, which represented the activation of NF-κB (Fig. 3B). Considering the high cytotoxicity of

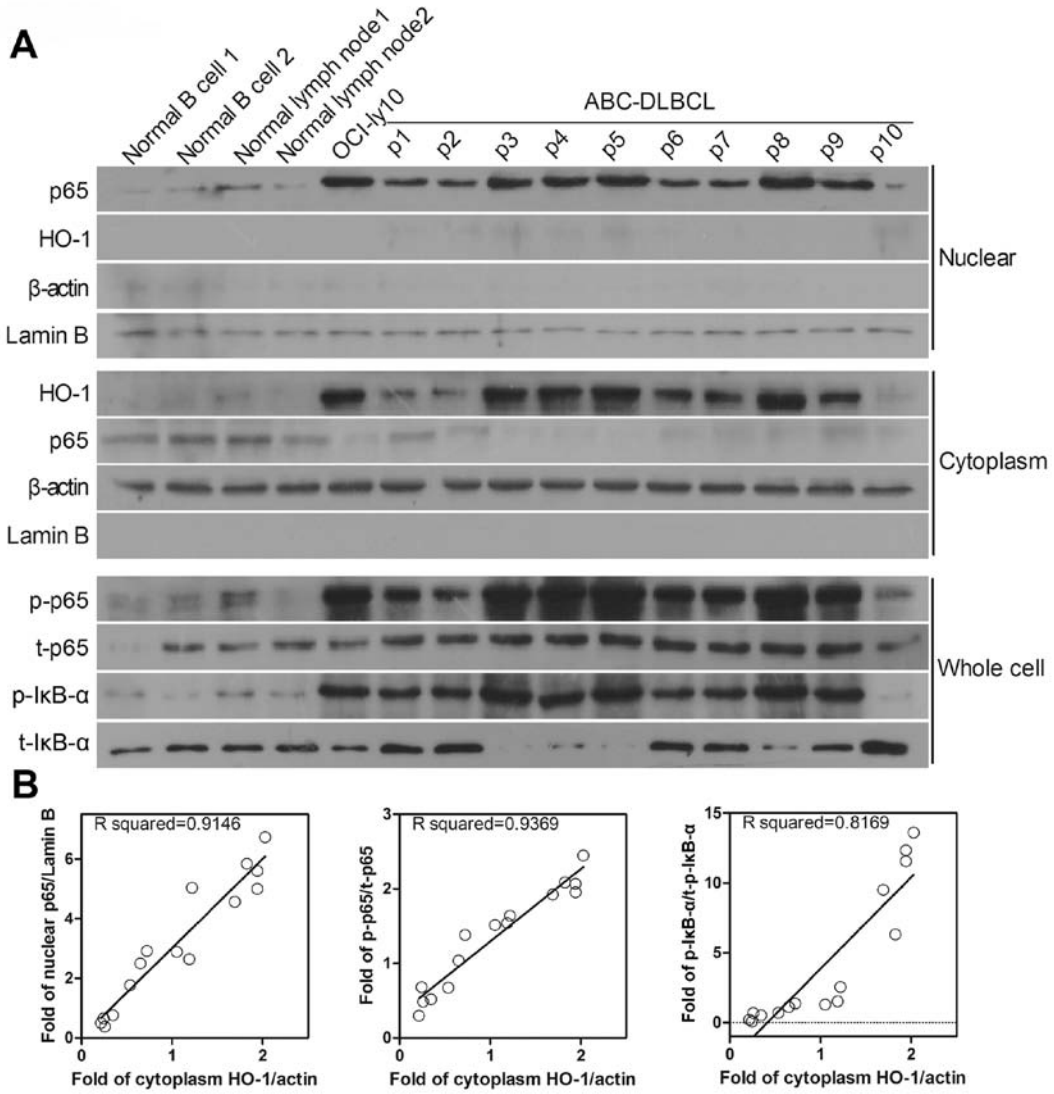

Figure 4. Protein levels of HO-1 and NF-κB are increased in ABC-DLBCL patients. (A) Nuclear and cytosolic western blots were reprobed for p65 and HO-1 expression. Whole-cell western blots were reprobed for p-IκB-α, p-p65, t-p65, and t-IκB-α expression. Lamin B was used as the nuclear protein reference whereas β-actin was used as the cytosolic and whole-cell protein references. (B) Scatterplot representing the correlation of HO-1 expression with the degree of NF-κB activation in ABC-DLBCL patient samples. For protein levels of nuclear p65 versus cytosolic HO-1 (B, left), the Spearman correlation coefficient R=0.9146, p<0.01; for protein levels of phosphorylated p65 versus cytosolic HO-1 (B, middle), R=0.9369, p<0.01; for protein levels of phosphorylated p-IκB-α versus cytosolic HO-1 (B, right), R=0.8169, p<0.01.

Bay11-7082 at a concentration of 15 μM (Fig. 3A), we finally chose the concentration of 10 μM to treat OCI-ly10 cells for 60 min. Then, western blot analysis of the protein levels of p-p65 and p-IκB-α readout of phosphorylation of IκB-α and p65) and HO-1, in different transduction groups untreated or treated with Bay11-7082, was performed. As shown in Fig. 3C, HO-1 expression could be inhibited by Bay11-7082 and siHO-1. Moreover, the combination of siHO-1 and Bay11-7082 significantly reduced HO-1 expression compared with the empty vector group. However, the expression of p-p65 and p-IκB-α was only slightly changed after silencing of HO-1 expression. Similarly, transduction of HO-1 had no effect on p-p65 and p-IκB-α. These results indicated that HO-1 was downstream of NF-κB.

The translocation of p65 is known to be an important indicator of NF-κB activation. Therefore, tumor necrosus factor-α (TNF-α) was used to activate the nuclear translocation of p65 in the absence and presence of Bay11-7082, which is also an NF-κB pharmacological inhibitor. In the absence of inhibitor, a significant response of p65 in the nucleus was obtained within 15 min. As shown in Fig. 3D and E, pretreatment with Bay11-7082 caused attenuation of the TNF-α-induced p65 translocation and HO-1 protein level in a concentration-dependent manner. In addition, Bay11-7082 decreased the HO-1 mRNA expression (Fig. 3F). Similarly, immunofluorescence staining showed that the TNF-α-induced translocation of p65 to the nucleus was blocked by pretreatment with Bay11-7082 (Fig. 3G). Double staining showed that the majority of HO-1 was localized in the cytoplasm of OCI-ly10 cells, where it was decreased while p65 was blocked. These results suggest that regulation of NF-κB can affect the expression of HO-1.

To further validate the results, 10 fresh tumor tissues from ABC-DLBCL patients were randomly selected and the NF-κB relative protein expression was analyzed (Fig. 4A). Cytosolic

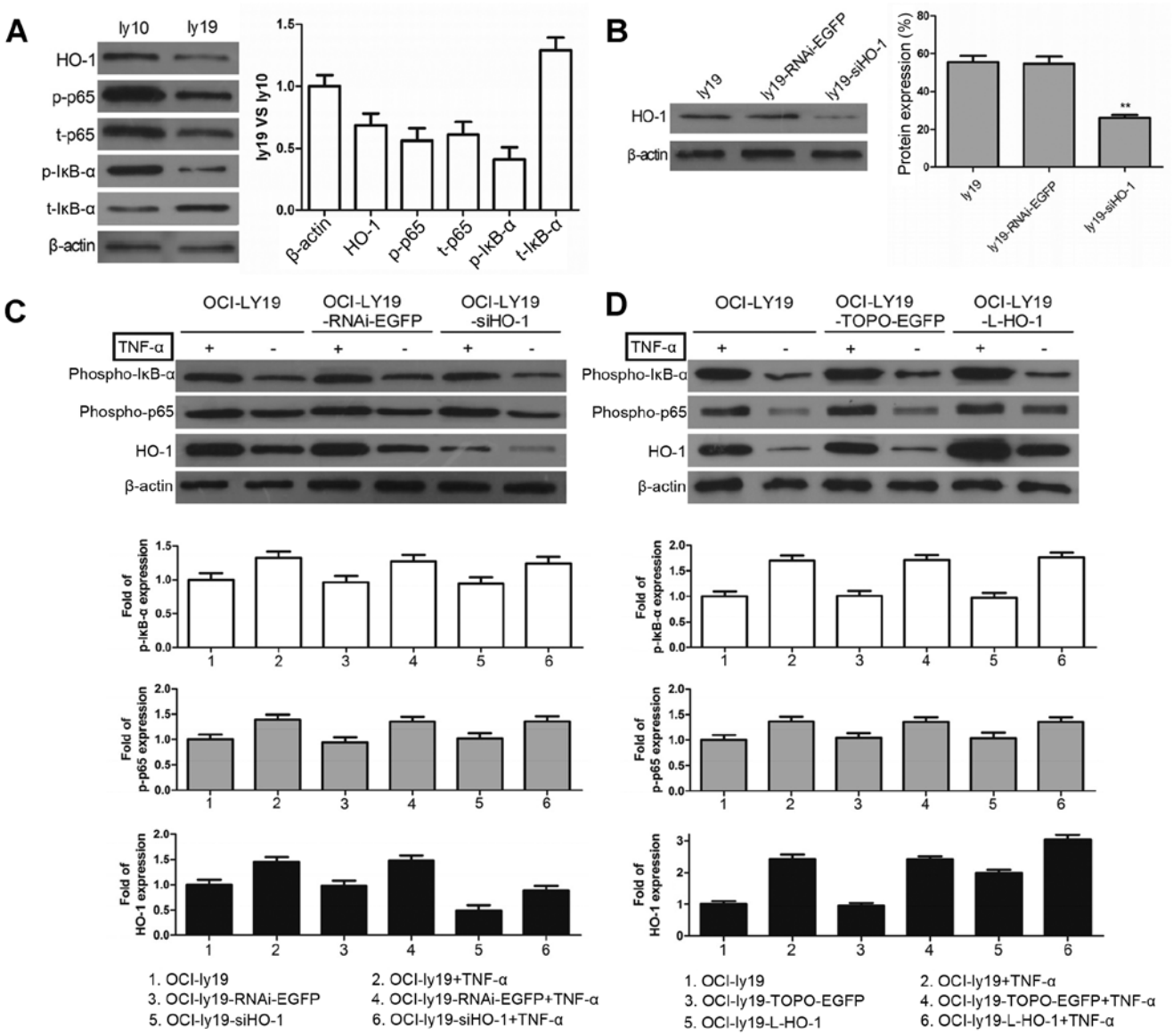

Figure 5. HO-1 is regulated by activated NF-κB in GCB-DLBCL. (A) Western blot analysis comparing the protein levels of HO-1 and NF-κB between the ABC-DLBCL-derived cell line OCI-ly10 and GCB-DLBCL-derived cell line OCI-ly19. (B) The OCI-ly19 cell line was transduced with lentivirus vectors and HO-1 was downregulated by L-U6.2-EGFP-siHO-1 (siHO-1). (C) OCI-ly19 cells were treated with control shRNA or HO-1 shRNA for 48 h and then treated with TNF-α alone or in combination with western blotting was used to measure HO-1, p-p65, and p-IκB-α expression. (D) OCI-ly19 cells were treated with L-TOPO-EGFP or L-TOPO-EGFP-HO-1 (L-HO-1) for 48 h and then treated with TNF-α alone or in combination with western blotting was used to measure the expression of HO-1, p-p65, and p-IκB-α.

HO-1 expression was positively correlated with nuclear p65 expression (R=0.9146) and with the phosphorylated forms of p65 and IκB-α, which were obtained from the whole-cell lysate (R=0.9369 and R=0.8169, respectively) (Fig. 4B). These results suggest that HO-1 expression is positively correlated with the degree of NF-κB activation in ABC-DLBCL. Moreover, it can be concluded that NF-κB is found upstream of HO-1 in ABC-DLBCL, regulating HO-1 expression and thereby affecting cell apoptosis.

Activated NF-κB-mediated upregulation of HO-1 expression inhibits apoptosis in GCB-DLBCL cells. Having shown that HO-1 overexpression is attributable to the constitutively activated NF-κB in ABC-DLBCL, we next wanted to determine whether activated NF-κB will cause changes in HO-1 expression in GCB-DLBCL cells that have low NF-κB activity (21). We compared the HO-1 expression and NF-κB activity levels in the ABC-DLBCL cell line OCI-ly10 with those in the GCB-DLBCL cell line OCI-ly19. The results showed that the aforementioned levels were lower in OCI-ly19 cells than in OCI-ly10 cells (Fig. 5A). We then used TNF-α to activate NF-κB and observed the HO-1 expression. After successfully knocking down HO-1 expression in OCI-ly19 cells with si-HO-1 (Fig. 5B), we incubated ly19, ly19-RNAi-EGFP, and ly19-siHO-1 with or without TNF-α. HO-1 expression was upregulated after the TNF-α-mediated increased phosphorylation of p65 and IκB-α (Fig. 5C). Furthermore, HO-1 expression was superinduced in the presence of both TNF-α and L-HO-1 (Fig. 5D). However, there was no effect on p-p65 and p-IκB-α when regulating HO-1 first. The results indicated that HO-1

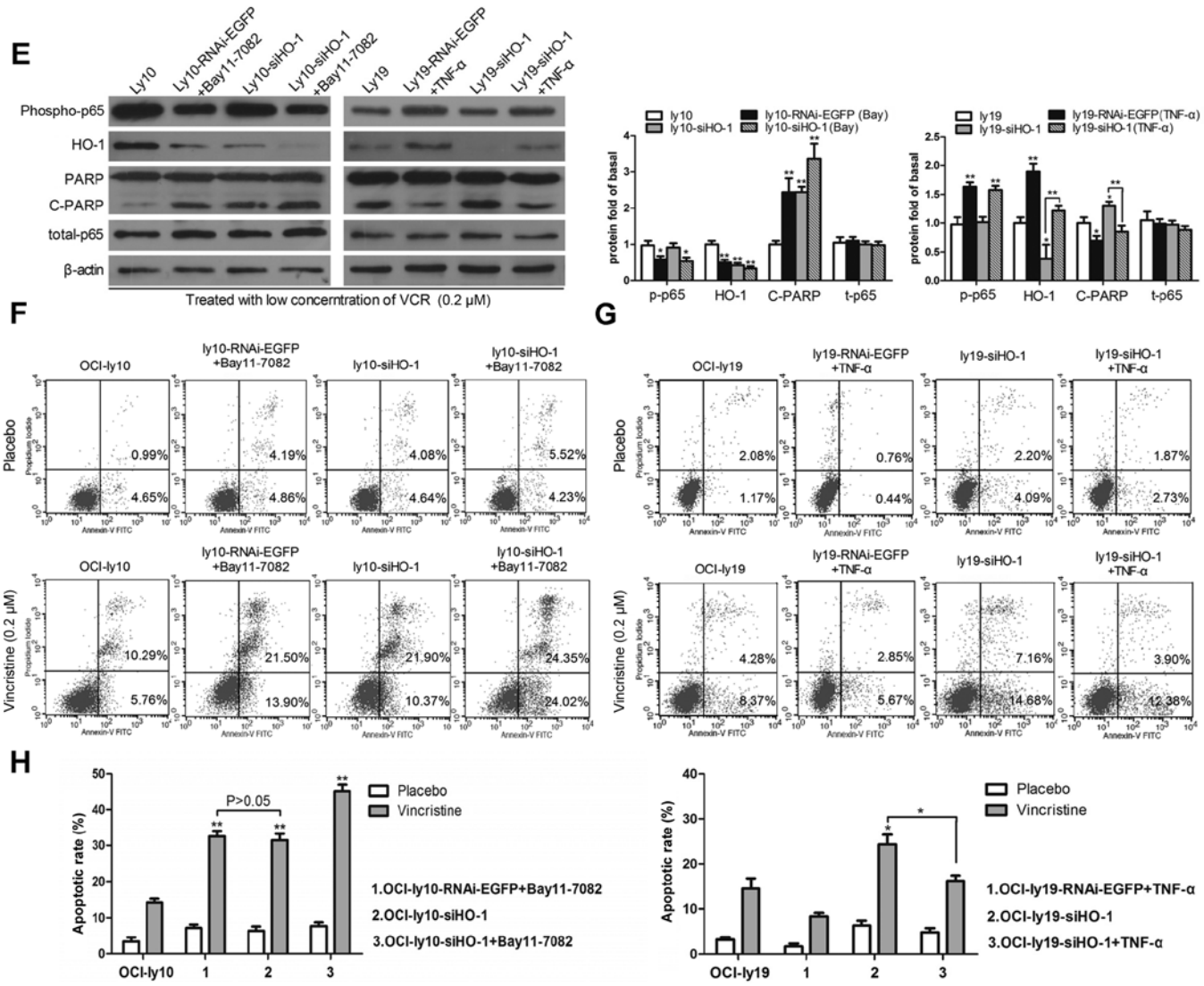

Figure 5. Continued. (E) Protein levels of HO-1, C-PARP, p-p65, and t-p65 were analyzed by western blotting. $^{**}p<0.01$ and $^{*}p<0.05$. (F) The apoptotic rate of transduced OCI-ly10 cells treated by HO-1 shRNA and Bay11-7082 was detected with flow cytometry. (G) The apoptosis rate of transduced OCI-ly19 cells treated by HO-1 shRNA and TNF-α was detected with flow cytometry. (H) The data statistics of apoptosis in transduced cells. All experiments were repeated 3 times. $^{**}p<0.01$ and $^{*}p<0.05$.

expression can be upregulated by NF-κB in GCB-DLBCL cells.

Poly(ADP-ribose) polymerase-1 (PARP-1), which can be proteolytically cleaved by caspase-3 at the DEVD peptide sequence site to generate an 85- and a 24-kDa fragment, is a known caspase-3 substrate. In OCI-ly10 cells, consistent with the decreased HO-1 protein levels, Bay11-7082 treatment or Lenti-siHO-1 expression increased the PARP cleavage activity, and their combination resulted in maximum cleavage of PARP (Fig. 5E). Furthermore, knockdown of HO-1 was associated with increased cleaved PARP in OCI-ly19 cells. However, such HO-1 decrease was reversed upon treatment with the NF-κB activator TNF-α.

Subsequently, apoptosis was detected in OCI-ly10 cells by flow cytometry, and the combination of Bay11-7082 and siHO-1 significantly increased the apoptotic event (Fig. 5F). However, there were no significant differences in apoptosis after either siHO-1 or Bay11-7082 treatment alone. In OCI-ly19 cells, the combination of TNF-α and siHO-1 could rescue the apoptotic phenotype caused by HO-1 silencing in OCI-ly19 cells (Fig. 5G). These results demonstrated that the NF-κB-mediated overexpression of HO-1 not only plays an anti-apoptotic role in ABC-DLBCL cells but also inhibits apoptosis in GCB-DLBCL cells. Thus, since HO-1 overexpression may be responsible for the dismal outcomes in ABC-DLBCL, a combined target comprising NF-κB and HO-1 may provide a new therapeutic option for this DLBCL subtype.

Discussion

HO-1 is well known as a stress-related cytoprotective molecule and is overexpressed in various tumors as well as hematological malignancies such as BCR-ABL-positive CML and most AMLs. Moreover, HO-1 overexpression is related to increased tumor proliferation and resistance to apoptosis. Currently, HO-1 has been confirmed as a novel target for AML and CML

(14,19). However, to the best of our knowledge, the relationship between HO-1 and DLBCL has not yet been elucidated. Thus, we focused on the expression of HO-1 and its role in DLBCL.

In this study, we showed that a high level of HO-1 expression is characteristic of the ABC lymphoma subtype. At the same time, HO-1 had a low level of expression in the GCB lymphoma subtype, but the expression was still significantly higher than that in normal lymph nodes due to the fact that HO-1 can be induced by various pathological stimuli. Analysis of the clinicopathological features possibly related to HO-1 showed that its high-level of expression was correlated with high levels of Ki-67 in DLBCL; this correlation was more obvious in ABC-DLBCL. Ki-67 is a nuclear antigen associated with tumor invasion and proliferation, and can be used as an index to judge the proliferation and malignancy degree of non-Hodgkin lymphoma (38). Miller *et al* demonstrated that a high proliferative index due to increased Ki-67 is inversely related with overall survival (39). Katzenberger *et al* demonstrated that the Ki-67 proliferation index is a quantitative indicator of clinical risk in mantle cell lymphoma (40). In the promotion of proliferation, Ki-67 and HO-1 have common points. Moreover, the rate of HO-1 positivity was significantly higher in patients with >1 site of extranodal involvement. These results suggest that, in addition to its widely known roles in tumor cells as a protective molecule against various stresses and in supporting rapid tumor growth, HO-1 may be associated with tumor invasion and proliferation.

Moreover, no significant association of HO-1 expression with other clinicopathological features of DLBCL was observed, including age, gender, performance status, IPI score, lactate dehydrogenase level, B symptoms, and T stage of tumors. However, it was observed that tissues of III/IV stage and with high-intermediate to high IPI scores showed higher levels of HO-1 expression. These results may be attributed to the use of a small number of patient samples.

Since HO-1 is overexpressed in ABC-DLBCL and may be associated with proliferation, we investigated the effect of high HO-1 expression on the ABC-DLBCL cell line OCI-ly10 after HO-1 overexpression or knockdown by lentiviral vector delivery. Despite incubation with DXM or VCR, HO-1 overexpression resulted in a higher viability rate and lower apoptotic rate. Moreover, HO-1 was negatively correlated with the cleaved forms of the caspase family of proteins. Numerous studies had reported that HO-1 overexpression plays an anti-apoptotic role and leads to drug resistance in hematological malignancies such as AML and CML (14,19). Our study demonstrated that HO-1 can also suppress apoptosis in ABC-DLBCL cells *in vitro*. Our next step would be to study the anti-apoptotic effect of HO-1 *in vivo*.

To date, several studies have indicated that NF-κB can regulate the induction of HO-1 expression (26-28). Li *et al* demonstrated that NF-κB activation is necessary for basal levels of cardiac HO-1 protein expression (29). We hypothesized that the high basal expression of HO-1 is due to NF-κB which is constitutively activated in ABC-DLBCL. NF-κB, a pathogenetic hallmark of ABC-DLBCL, promotes cell survival and proliferation and inhibits apoptosis (2). In this study, activated NF-κB increased the expression of HO-1, whereas NF-κB inhibition had the opposite effect. Expression of p-p65 and p-IκB-α was not affected by the changes in HO-1, and this verified that HO-1 is directly downstream of NF-κB. On comparing the protein levels of NF-κB and HO-1 in 10 randomly selected patients of ABC-DLBCL and control groups, we found that HO-1 was constitutively activated in ABC-DLBCLs. Furthermore, phosphorylation of the NF-κB subunit p65 and of IκB-α may be responsible for the expression of HO-1.

Further studies were performed on the GCB-DLBCL-derived cell line OCI-ly19 that has a low level of NF-κB activity. After the TNF-α-mediated activation of NF-κB, increased HO-1 expression was observed. Taken together, these results show that basal HO-1 expression is under the control of NF-κB. Moreover, if the basal NF-κB activity is stimulated in OCI-ly19 cells, HO-1 will be subsequently induced and therefore provides a second line of defense against anticancer drugs. However, combining the inhibition of NF-κB and HO-1 in OCI-ly10 cells significantly increased apoptosis and thus may suggest a new target for therapy of ABC-DLBCL.

A bigger sample pool of DLBCL patients is required to perform further investigations to verify HO-1 expression in different DLBCL subtypes. The underlying signaling pathway remains to be further elucidated since the mechanism of how HO-1 overcomes apoptosis is unclear.

In conclusion, the characteristic overexpression of HO-1 is mediated by constitutively activated NF-κB in ABC-DLBCL. HO-1 expression inhibits apoptosis in ABC-DLBCL, whereas HO-1 silencing promotes apoptosis. Increasing the expression of HO-1 in GCB-DLBCL-derived OCI-ly19 cells can lead to drug resistance. Furthermore, the combination of NF-κB and HO-1 may provide a new target for the therapy of ABC-DLBCL. The findings herein provide valuable experimental evidence for the targeted therapy of ABC-DLBCL.

Acknowledgements

This study was supported, in part, by the National Natural Science Foundation of China (Nos. 81070444, 81270636, 81360501 and 81470006), International Cooperation Project of Guizhou Province (No. 2011-7010), Social Project of Guizhou Province (No. 2011-3012), Provincial Government Special Fund of Guizhou Province (No. 2010-84), Science and Technology Foundation of Guizhou Province (J word[2010]-2164), Union Project of Guizhou Province Science and Technology (LH word, [2015]-7386) and Project of Science and Technology Bureau of Guiyang City (No. 2012103-36).

References

1. World Health Organization Classification of Tumors of Haematopoietic and Lymphoid Tissues. IARC Press, Lyon, 2008.
2. Nogai H, Dörken B and Lenz G: Pathogenesis of non-Hodgkin's lymphoma. J Clin Oncol 29: 1803-1811, 2011.
3. Alizadeh AA, Eisen MB, Davis RE, Ma C, Lossos IS, Rosenwald A, Boldrick JC, Sabet H, Tran T, Yu X, *et al*: Distinct types of diffuse large B-cell lymphoma identified by gene expression profiling. Nature 403: 503-511, 2000.
4. Lenz G, Wright G, Dave SS, Xiao W, Powell J, Zhao H, Xu W, Tan B, Goldschmidt N, Iqbal J, *et al*; Lymphoma/Leukemia Molecular Profiling Project: Stromal gene signatures in large-B-cell lymphomas. N Engl J Med 359: 2313-2323, 2008.
5. Jozkowicz A, Was H and Dulak J: Heme oxygenase-1 in tumors: Is it a false friend? Antioxid Redox Signal 9: 2099-2117, 2007.

6. Foresti R, Clark JE, Green CJ and Motterlini R: Thiol compounds interact with nitric oxide in regulating heme oxygenase-1 induction in endothelial cells. Involvement of superoxide and peroxynitrite anions. J Biol Chem 272: 18411-18417, 1997.
7. Stuhlmeier KM: Activation and regulation of Hsp32 and Hsp70. Eur J Biochem 267: 1161-1167, 2000.
8. Terry CM, Clikeman JA, Hoidal JR and Callahan KS: Effect of tumor necrosis factor-alpha and interleukin-1 alpha on heme oxygenase-1 expression in human endothelial cells. Am J Physiol 274: H883-H891, 1998.
9. Miyazaki T, Kirino Y, Takeno M, Samukawa S, Hama M, Tanaka M, Yamaji S, Ueda A, Tomita N, Fujita H, *et al*: Expression of heme oxygenase-1 in human leukemic cells and its regulation by transcriptional repressor Bach1. Cancer Sci 101: 1409-1416, 2010.
10. Furfaro AL, Piras S, Passalacqua M, Domenicotti C, Parodi A, Fenoglio D, Pronzato MA, Marinari UM, Moretta L, Traverso N, *et al*: HO-1 up-regulation: A key point in high-risk neuroblastoma resistance to bortezomib. Biochim Biophys Acta 1842: 613-622, 2014.
11. Lee SE, Yang H, Jeong SI, Jin YH, Park CS and Park YS: Induction of heme oxygenase-1 inhibits cell death in crotonaldehyde-stimulated HepG2 cells via the PKC-δ-p38-Nrf2 pathway. PLoS One 7: e41676, 2012.
12. Zhang L, Liu YL, Chen GX, Cui B, Wang JS, Shi YL, Li LP and Guo XB: Heme oxygenase-1 promotes Caco-2 cell proliferation and migration by targeting CTNND1. Chin Med J (Engl) 126: 3057-3063, 2013.
13. Kongpetch S, Kukongviriyapan V, Prawan A, Senggunprai L, Kukongviriyapan U and Buranrat B: Crucial role of heme oxygenase-1 on the sensitivity of cholangiocarcinoma cells to chemotherapeutic agents. PLoS One 7: e34994, 2012.
14. Mayerhofer M, Gleixner KV, Mayerhofer J, Hoermann G, Jaeger E, Aichberger KJ, Ott RG, Greish K, Nakamura H, Derdak S, *et al*: Targeting of heat shock protein 32 (Hsp32)/heme oxygenase-1 (HO-1) in leukemic cells in chronic myeloid leukemia: A novel approach to overcome resistance against imatinib. Blood 111: 2200-2210, 2008.
15. Ma D, Fang Q, Wang P, Gao R, Sun J, Li Y, Hu XY and Wang JS: Downregulation of HO-1 promoted apoptosis induced by decitabine via increasing p15INK4B promoter demethylation in myelodysplastic syndrome. Gene Ther 22: 287-296, 2015.
16. Wei S, Wang Y, Chai Q, Fang Q, Zhang Y and Wang J: Potential crosstalk of Ca^{2+}-ROS-dependent mechanism involved in apoptosis of Kasumi-1 cells mediated by heme oxygenase-1 small interfering RNA. Int J Oncol 45: 2373-2384, 2014.
17. Ma D, Fang Q, Wang P, Gao R, Wu W, Lu T, Cao L, Hu X and Wang J: Induction of heme oxygenase-1 by Na^{+}-H^{+} exchanger 1 protein plays a crucial role in imatinib-resistant chronic myeloid leukemia cells. J Biol Chem 290: 12558-12571, 2015.
18. Wang P, Ma D, Wang J, Fang Q, Gao R, Wu W, Lu T and Cao L: Silencing HO-1 sensitizes SKM-1 cells to apoptosis induced by low concentration 5-azacytidine through enhancing p16 demethylation. Int J Oncol 46: 1317-1327, 2015.
19. Lin X, Fang Q, Chen S, Zhe N, Chai Q, Yu M, Zhang Y, Wang Z and Wang J: Heme oxygenase-1 suppresses the apoptosis of acute myeloid leukemia cells via the JNK/c-JUN signaling pathway. Leuk Res 39: 544-552, 2015.
20. Davis RE, Brown KD, Siebenlist U and Staudt LM: Constitutive nuclear factor kappaB activity is required for survival of activated B cell-like diffuse large B cell lymphoma cells. J Exp Med 194: 1861-1874, 2001.
21. Compagno M, Lim WK, Grunn A, Nandula SV, Brahmachary M, Shen Q, Bertoni F, Ponzoni M, Scandurra M, Califano A, *et al*: Mutations of multiple genes cause deregulation of NF-kappaB in diffuse large B-cell lymphoma. Nature 459: 717-721, 2009.
22. Davis RE, Ngo VN, Lenz G, Tolar P, Young RM, Romesser PB, Kohlhammer H, Lamy L, Zhao H, Yang Y, *et al*: Chronic active B-cell-receptor signalling in diffuse large B-cell lymphoma. Nature 463: 88-92, 2010.
23. Lenz G and Staudt LM: Aggressive lymphomas. N Engl J Med 362: 1417-1429, 2010.
24. Ngo VN, Davis RE, Lamy L, Yu X, Zhao H, Lenz G, Lam LT, Dave S, Yang L, Powell J, *et al*: A loss-of-function RNA interference screen for molecular targets in cancer. Nature 441: 106-110, 2006.
25. Lam LT, Davis RE, Pierce J, Hepperle M, Xu Y, Hottelet M, Nong Y, Wen D, Adams J, Dang L, *et al*: Small molecule inhibitors of IkappaB kinase are selectively toxic for subgroups of diffuse large B-cell lymphoma defined by gene expression profiling. Clin Cancer Res 11: 28-40, 2005.
26. Lavrovsky Y, Schwartzman ML, Levere RD, Kappas A and Abraham NG: Identification of binding sites for transcription factors NF-kappa B and AP-2 in the promoter region of the human heme oxygenase 1 gene. Proc Natl Acad Sci USA 91: 5987-5991, 1994.
27. Kurata S, Matsumoto M, Tsuji Y and Nakajima H: Lipopolysaccharide activates transcription of the heme oxygenase gene in mouse M1 cells through oxidative activation of nuclear factor kappa B. Eur J Biochem 239: 566-571, 1996.
28. Lin CC, Chiang LL, Lin CH, Shih CH, Liao YT, Hsu MJ and Chen BC: Transforming growth factor-beta1 stimulates heme oxygenase-1 expression via the PI3K/Akt and NF-kappaB pathways in human lung epithelial cells. Eur J Pharmacol 560: 101-109, 2007.
29. Li Q, Guo Y, Ou Q, Cui C, Wu WJ, Tan W, Zhu X, Lanceta LB, Sanganalmath SK, Dawn B, *et al*: Gene transfer of inducible nitric oxide synthase affords cardioprotection by upregulating heme oxygenase-1 via a nuclear factor-{kappa}B-dependent pathway. Circulation 120: 1222-1230, 2009.
30. Rushworth SA, Zaitseva L, Murray MY, Shah NM, Bowles KM and MacEwan DJ: The high Nrf2 expression in human acute myeloid leukemia is driven by NF-κB and underlies its chemoresistance. Blood 120: 5188-5198, 2012.
31. Ogborne RM, Rushworth SA and O'Connell MA: Alpha-lipoic acid-induced heme oxygenase-1 expression is mediated by nuclear factor erythroid 2-related factor 2 and p38 mitogen-activated protein kinase in human monocytic cells. Arterioscler Thromb Vasc Biol 25: 2100-2105, 2005.
32. Rushworth SA, Chen XL, Mackman N, Ogborne RM and O'Connell MA: Lipopolysaccharide-induced heme oxygenase-1 expression in human monocytic cells is mediated via Nrf2 and protein kinase C. J Immunol 175: 4408-4415, 2005.
33. Ai ZL, Zhu CH, Min M, Wang J, Lan CH, Fan LL, Sun WJ and Chen DF: The role of hepatic liver X receptor α- and sterol regulatory element binding protein-1c-mediated lipid disorder in the pathogenesis of non-alcoholic steatohepatitis in rats. J Int Med Res 39: 1219-1229, 2011.
34. Scott DW, Wright GW, Williams PM, Lih CJ, Walsh W, Jaffe ES, Rosenwald A, Campo E, Chan WC, Connors JM, *et al*: Determining cell-of-origin subtypes of diffuse large B-cell lymphoma using gene expression in formalin-fixed paraffin-embedded tissue. Blood 123: 1214-1217, 2014.
35. Gandini NA, Fermento ME, Salomón DG, Blasco J, Patel V, Gutkind JS, Molinolo AA, Facchinetti MM and Curino AC: Nuclear localization of heme oxygenase-1 is associated with tumor progression of head and neck squamous cell carcinomas. Exp Mol Pathol 93: 237-245, 2012.
36. Miyata Y, Kanda S, Mitsunari K, Asai A and Sakai H: Heme oxygenase-1 expression is associated with tumor aggressiveness and outcomes in patients with bladder cancer: A correlation with smoking intensity. Transl Res 164: 468-476, 2014.
37. Gerdes J, Schwab U, Lemke H and Stein H: Production of a mouse monoclonal antibody reactive with a human nuclear antigen associated with cell proliferation. Int J Cancer 31: 13-20, 1983.
38. Szczuraszek K, Mazur G, Jeleń M, Dziegiel P, Surowiak P and Zabel M: Prognostic significance of Ki-67 antigen expression in non-Hodgkin's lymphomas. Anticancer Res 28A: 1113-1118, 2008.
39. Miller TP, Grogan TM, Dahlberg S, Spier CM, Braziel RM, Banks PM, Foucar K, Kjeldsberg CR, Levy N, Nathwani BN, *et al*: Prognostic significance of the Ki-67-associated proliferative antigen in aggressive non-Hodgkin's lymphomas: A prospective Southwest Oncology Group trial. Blood 83: 1460-1466, 1994.
40. Katzenberger T, Petzoldt C, Höller S, Mäder U, Kalla J, Adam P, Ott MM, Müller-Hermelink HK, Rosenwald A and Ott G: The Ki67 proliferation index is a quantitative indicator of clinical risk in mantle cell lymphoma. Blood 107: 3407, 2006.